2003

Evolving Spectra of Population III Stars: Consequences for Cosmological Reionization

Aparna Venkatesan
University of San Francisco, avenkatesan@usfca.edu

Jason Tumlinson

J Shull

Follow this and additional works at: http://repository.usfca.edu/phys

Part of the Astrophysics and Astronomy Commons, and the Physics Commons

EVOLVING SPECTRA OF POPULATION III STARS: CONSEQUENCES FOR COSMOLOGICAL REIONIZATION

Aparna Venkatesan,[1] Jason Tumlinson,[2] and J. Michael Shull[3]

Center for Astrophysics and Space Astronomy, Department of Astrophysical and Planetary Sciences, UCB 389, University of Colorado, Boulder, CO 80309-0389; aparna@casa.colorado.edu, tumlinso@casa.colorado.edu, mshull@casa.colorado.edu

ABSTRACT

We examine the significance of the first metal-free stars (Population III) for the cosmological reionization of H I and He II. These stars have unusually hard spectra, with the integrated ionizing photon rates from a Population III stellar cluster for H I and He II being 1.6 and 10^5 times stronger, respectively, than those from a Population II cluster. For the currently favored cosmology, we find that Population III stars alone can reionize H I at redshifts of $z \simeq 9$ and 4.7 and He II at $z \simeq 5.1$ and 0.7 for continuous and instantaneous modes of star formation, respectively. More realistic scenarios involving combinations of Population III and Population II stellar spectra yield similar results for hydrogen. Helium never reionizes completely in these cases; the ionization fraction of He III reaches a maximum of about 60% at $z \sim 5.6$ if Population III star formation lasts for 10^9 yr. Future data on H I reionization can test the amount of small-scale power available to the formation of the first objects and provide a constraint on values of $\sigma_8 \lesssim 0.7$. Since current UV observations indicate an epoch of reionization for He II at $z \sim 3$, He II may reionize more than once. Measurements of the He II Gunn-Peterson effect in the intergalactic medium at redshifts $z \gtrsim 3$ may reveal the significance of Population III stars for He II reionization, particularly in "void" regions that may contain "relic" ionization from early Population III stellar activity.

Subject headings: cosmology: theory — intergalactic medium

1. INTRODUCTION

The nature, formation sites, and epochs of the first stars in the universe are some of cosmology's most intriguing yet unresolved questions today. Theoretical studies of the effects of these objects on the high-redshift intergalactic medium (IGM) and on galaxy formation have a rapidly expanding literature, driven in part by the potential to test the predictions from such theories with data in the near future. Recent work on the first stars has focused on signatures such as the effects of stellar radiation and nucleosynthesis on their host galaxies and the IGM (Gnedin & Ostriker 1997; Haiman & Loeb 1997; Ferrara, Pettini, & Shchekinov 2000; Abia et al. 2001; Ricotti, Gnedin, & Shull 2002)—loosely grouped under stellar and supernova (SN) feedback—and the potential presence of large numbers of stellar remnants in galactic halos in baryonic dark matter scenarios (Fields, Freese, & Graff 1998). These studies have been directly motivated by observations of the reionization (Becker et al. 2001; Kriss et al. 2001) and trace metal enrichment (Songaila 2001) of the high-z IGM and the detection of solar-mass dark objects in our Galactic halo by microlensing experiments (Alcock et al. 2000). Although it is unclear if the same population of early stars can be tied unambiguously to all of these data, it is likely that they contributed significantly to the ionizing photon budget and metal production at early times.

Beyond such signatures, there has also been considerable interest in the typical masses of the first stars and the preferred environments, if any, in which they form. There is no theoretical basis on which one can a priori rule out a stellar initial mass function (IMF) that was different in the past. Indeed, arguments for a primordial IMF biased toward higher masses have been proposed for some time (Carr, Bond, & Arnett 1984; Larson 1998; Abel, Bryan, & Norman 2000; Hernandez & Ferrara 2001; Bromm, Kudritzki, & Loeb 2001; Nakamura & Umemura 2002), although there is no indication for an environment-dependent IMF from data from a variety of local star-forming regions (Kroupa 2002). As for the nature of the typical galaxy that hosts the first stars, this depends critically on the availability of coolants within virialized halos so that the fragmentation necessary for star formation can commence. Several authors (Tegmark et al. 1997; Ciardi et al. 2000) have argued that modest levels of early stellar activity can generate sufficient far-ultraviolet radiation in the Lyman-Werner bands (11.2–13.6 eV) to photodissociate all of the remaining H_2 in the universe, well before the associated H I ionizing flux has built up to values sufficient for reionization. A long pause in global star formation would then ensue, owing to "negative feedback," and star formation would resume only when halos of virial temperature $\gtrsim 10^4$ K collapse, corresponding to the threshold for the onset of H-line cooling. One way to overcome such negative feedback might be through the presence of X-rays or ionizing UV photons from the first luminous sources, which could boost the free electron fraction and hence the amount of H^--catalyzed H_2, leading to a compensatory positive feedback (Ricotti, Gnedin, & Shull 2001). It remains unclear how effective this is in overcoming the negative feedback from infrared and Lyman-Werner band photons (Haiman, Abel, & Rees 2000; Venkatesan, Giroux, & Shull 2001). There is also the possibility that sufficient metals are injected into the interstellar medium (ISM) soon after the very first stars form. In this case, the

distinction between halos cooling by H_2 versus H becomes irrelevant, assuming that the metals can be retained in the cold star-forming gaseous component within individual halos. This problem remains unresolved currently, but it is clear that the chemistry of high-z halos is critical to when and where the first stars formed.

A priori, we would expect early generations of stars forming from primordial gas to be metal-free in composition, although no surviving members of such populations have been detected to date. Recent studies of stars of zero metallicity Z (Tumlinson & Shull 2000; Bromm et al. 2001; Cojazzi et al. 2000; Schaerer 2002 and references therein), which we hereafter refer to as Population III, have demonstrated that $Z = 0$ stars are fundamentally different in nature and evolutionary properties from their low-Z counterparts. In particular, Tumlinson & Shull (2000) showed, in a calculation of the zero-age main sequence (ZAMS) of these stars, that their harder ionizing spectra could be relevant for both the H I and He II reionization of the IGM. This work has subsequently been extended to full calculations of the evolving spectra of Population III stellar populations in Tumlinson et al. (2003; hereafter Paper I), where we find that, for a Salpeter IMF, the integrated ionizing photon rate from a Population III cluster for H I and He II is 1.6 and 10^5 times stronger, respectively, than that for a $Z = 0.001$ cluster (Leitherer et al. 1999) of the same mass.[4] In Paper I, we examine the evolving spectra of Population III stars and their observational signatures such as broadband colors and emission lines. In the present paper, which is intended as a companion work to Paper I, we focus on the significance of such metal-free stellar populations for cosmological reionization, under the assumption that they form in a present-day IMF.

We present a brief review here of the status of theoretical models and data on reionization. Spectroscopic studies of high-z quasars and galaxies blueward of their rest-frame H I and He II Lyα emission have revealed that He II reionization occurs at $z \sim 3$ (Kriss et al. 2001) and that of H I before $z \sim 6$ (Becker et al. 2001). Such spectroscopic observations, along with increasingly precise data on the cosmic microwave background (CMB), are beginning to place strong complementary bounds on the redshift of H I reionization $z_{\mathrm{reion,H}}$. At one end, current CMB data on the temperature anisotropy at degree and subdegree scales provide an upper limit of about 0.3 for the electron-scattering optical depth to reionization, which may be translated into a model-dependent constraint of $z_{\mathrm{reion,H}} \lesssim 25$ (Wang, Tegmark, & Zaldarriaga 2002). Ongoing and future CMB observations[5] will provide improved constraints on $z_{\mathrm{reion,H}}$ through the detection of polarization in the CMB at large angular scales (Staggs & Church 2001). At the other end of the range for $z_{\mathrm{reion,H}}$, the IGM appears to be highly ionized up to $z \sim 6$ (Fan et al. 2000; Dey et al. 1998). Becker et al. (2001)

recently detected the H I Gunn-Peterson (GP) trough in the spectrum of the highest redshift quasar known to date at $z = 6.28$ (Fan et al. 2001), which may indicate that H I reionization occurs not far beyond $z \sim 6$. This claim has been challenged, however, by the subsequent observation of Lyα emission in a $z = 6.56$ galaxy (Hu et al. 2002). The extent to which this Lyα emission line has been eroded by the damping wing of Lyα absorption in the IGM (Miralda-Escudé 1998) is, however, unclear. It is therefore difficult to assess whether H I reionization is complete at $z \sim 6.5$ based on this one object. Although the detection of the GP trough in a single line of sight is not definitive evidence of the global reionization of the IGM, it may probe the end of the gradual process of inhomogeneous reionization, coinciding with the disappearance of the last neutral regions in the high-z IGM. Reionization of H I at $z \sim 6$–9 would still be consistent with the lower end of the range of redshifts, $z \sim 6$–20, predicted by theoretical models, both semianalytic (Tegmark, Silk, & Blanchard 1994; Giroux & Shapiro 1996; Haiman & Loeb 1997; Valageas & Silk 1999; Madau, Haardt, & Rees 1999; Miralda-Escudé, Haehnelt, & Rees 2000) and based on numerical simulations (Cen & Ostriker 1993; Gnedin 2000; Ciardi et al. 2000; Benson et al. 2002).

The reionization of the IGM subsequent to recombination at $z \sim 1000$ is thought to have been caused by increasing numbers of the first luminous sources. Although there are a variety of models for the astrophysical objects or processes that could have reionized the IGM, the leading scenarios involve photoionization by sources with soft or hard ionizing spectra, or equivalently, stellar-type or QSO-type models, respectively. Clearly, this division of source populations according to their spectral properties is no longer valid if the first stars generated hard ionizing radiation by virtue of their metal-free composition (Paper I) or if they formed in an IMF biased toward extremely high masses (Bromm et al. 2001). The large majority of currently favored reionization models involve stars rather than QSOs, for a number of observationally motivated reasons (see Venkatesan 2002 for a detailed discussion on this point). These reasons include the apparent decrease in the space density of large, optically bright quasars up to $z \sim 6.3$, beyond a peak at $z \sim 3$ (Fan et al. 2001; Shaver et al. 1999), so that their UV and X-ray photons are insufficient for H I reionization (Madau 1998; Venkatesan et al. 2001). However, the nature of the reionizing sources is highly uncertain at present, and one can neither confirm nor exclude stars, faint QSOs ("mini-QSOs"), or a combination of high-z source populations. In this paper, we are not specifically advocating that Population III stars are solely responsible for reionization. Rather, our main goal is to examine the consequences of an epoch of metal-free star formation for the H I and He II reionization of the IGM, given a model of reionization with currently favored values for the input parameters.

We organize the paper as follows: In § 2 we present the newly calculated evolving spectra of Population III from Paper I, and we describe the reionization model used in the present work. In § 3 we present our results on the effects of Population III and Population II stars on the H I and He II reionization of the IGM for a number of potential scenarios of high-z star formation. We also discuss the potential constraint offered by the reionization epoch on the amount of small-scale power in structure formation models, and we speculate on the fate of partially or fully ionized He III in underdense regions of the IGM whose detection lies on

---

[4] In this comparison, we do not include the contribution of Wolf-Rayet stars, which can boost the ionizing radiation from a Population II stellar cluster. In fact, the existence of the Wolf-Rayet phase in $Z = 0$ stars is questionable, as discussed in Paper I, given that these objects are unlikely to experience strong mass loss. We are primarily interested here in a direct comparison of the ionizing radiation from the main-sequence phases of Populations III and II.

[5] See http://www.hep.upenn.edu/~max/cmb/experiments.html and http://background.uchicago.edu/~whu/cmbex.html for links to various CMB experiments.

the threshold of current capabilities. We present our conclusions in § 4.

2. THE REIONIZATION MODEL

We use the semianalytic stellar reionization model described in Venkatesan (2000, hereafter V2000) and consider only the effects of stars. This model calculates the fraction of baryons in collapsed halos with the Press-Schechter formulation and, given a prescription for star formation and the generated ionizing radiation, tracks the hydrogen and helium reionization of the IGM. We adopt the methods developed in V2000, replacing the standard cold dark matter (SCDM) model of V2000 with a ΛCDM cosmology, and we significantly improve the solution for the growth of ionization regions around individual halos, as described below.

We take the primordial matter power spectrum of density fluctuations to be $P(k) \propto k^n T^2(k)$, where n is the index of the scalar power spectrum and the matter transfer function $T(k)$ is taken from Eisenstein & Hu (1998). We assume that there are no tensor contributions to $P(k)$. We normalize $P(k)$ to the present-day rms density contrast σ_8 over spheres of radius $8 \, h^{-1}$ Mpc, in which we assume that the bias factor is unity (i.e., that light traces the underlying mass distribution). We choose this normalization rather than the *COBE* normalization from the CMB, since the physical scales associated with σ_8 are relatively close to those relevant for reionization and the formation of the first luminous objects.

We track the fraction F_B of all baryons in collapsed dark matter halos by the Press-Schechter formalism, allowing star formation only in massive halos of virial temperature $\gtrsim 10^4$ K, corresponding to the mass threshold for the onset of hydrogen-line cooling. In the absence of metals, H is likely to be the primary coolant, since H_2 is easily destroyed by trace levels of stellar UV radiation. In the case of low-mass halos, the interplay between positive and negative feedback on H_2 formation and destruction can lead to time-varying H_2 abundances. This in turn causes episodic star formation, so that the generated ionization fronts (I-fronts) remain trapped in the host galaxy and do not have a large effect on the IGM (Ricotti et al. 2002). We therefore focus on reionization from high-mass halos.

We assume that the fraction of baryons in each galaxy halo forming stars is given by f_* and that the fractions of H I and He II ionizing photons escaping from individual halos are given by f_{esc}^H and f_{esc}^{He}, respectively. Our assumed values for these parameters are discussed below. We assume that the ionizing photons propagate isotropically from their host galaxies into the IGM, generating an ionized sphere around each source of radius r_i. We solve for the size of the ionized regions associated with each such star-forming galaxy, which, when integrated over all halos, yields at each redshift the volume filling factor of H II ($F_{H II}$) or He III ($F_{He III}$). Reionization is defined as the epoch when individual ionized regions overlap, when $F_{H II} = 1$ or $F_{He III} = 1$; we return to this below.

Since most cosmological parameters are becoming increasingly well constrained by combined CMB, large-scale structure, and high-z SN Ia observations, the remaining uncertainty in the "initial conditions" for reionization rests largely with σ_8 and, to a lesser degree, on n. The scalar power spectrum index is currently measured by the above techniques to about 10% error, $n \sim 0.9$–1.1. The data on σ_8 are currently divided between two values, one at about 0.9–

1.0 (Evrard et al. 2002; Refregier, Rhodes, & Groth 2002), and the other at a substantially lower value of about 0.7 (Reiprich & Böhringer 2002). We choose $\sigma_8 = 0.9$ in this work as a representative intermediate value. We caution that σ_8 can be reduced in value only to a certain degree in reionization models; otherwise, there is a significant loss of power on small scales, which may lead to reionization too late to be consistent with current data. Some leverage can be regained by increasing n or by fine-tuning the astrophysical parameters in the model, but this may not prove sufficient. We return to this topic in § 3.3.

We set $f_* = 0.05$ for all galaxy halos. This value is consistent with the findings of numerical simulations of star formation in early halos and with the constraint of avoiding the overenrichment of the IGM in metals by $z \sim 3$ (see V2000 and references therein), for both continuous and bursting modes of star formation. We set $f_{esc}^H = 0.05$ (Deharveng et al. 2001; Dove, Shull, & Ferrara 2000; Leitherer et al. 1995) to be consistent with data from the local universe, particularly from high-mass systems, and assuming that local systems describe the conditions found in the first star-forming galaxies. Although observations of Lyman continuum emission from Lyman break galaxies at $z \sim 3.4$ by Steidel, Pettini, & Adelberger (2001) indicate values of f_{esc}^H exceeding 0.5, it is not clear how representative these systems are of high-z star formation and how much these high values are an artifact of the observational procedure.

Assigning a value to f_{esc}^{He} for individual galaxies is somewhat more uncertain. Given the greater recombination rate of He III relative to H II and the fact that most astrophysical sources have much lower He II ionizing fluxes relative to the values for H I, one would expect f_{esc}^{He} to be lower than f_{esc}^H. On the other hand, a combination of the first wave of ionizing photons and the clearing of the ISM in high-z galaxies by the first SNe may provide "equal-opportunity chimneys" for the escape of H I and He II ionizing photons. Given the lack of data on f_{esc}^{He} and the above factors, we set $f_{esc}^{He} = 0.5 f_{esc}^H = 0.025$ as a reasonable first guess at this quantity; certainly, we do not expect f_{esc}^{He} to exceed f_{esc}^H. Although we have adopted reasonable values for these astrophysical parameters, they are likely to have some dependence on redshift and individual galaxy masses; thus, the assumption of a constant value for them is an oversimplification. However, the relevant issue is that they have to combine in such a way as to be consistent with the above constraints and lead, for most reionization models, to H II and He III reionization at epochs consistent with those from observations.

We include the effects of inhomogeneity in the IGM through a clumping factor c_L, rather than assuming a smooth IGM as in V2000. We define c_L to be the space-averaged clumping factor of photoionized hydrogen or helium, $c_L \equiv \langle n_i^2 \rangle / \langle n_i \rangle^2$, where i corresponds to H II or He III. Here we take c_L to be the same for both H II and He III. The parameter c_L can affect the epoch of reionization significantly, with higher values leading to delayed reionization. However, within a specific framework of cosmology and structure evolution, c_L is a derived rather than an independent parameter. Although c_L is necessarily redshift dependent, we assume $c_L = 30$, which is a reasonable average from, e.g., Madau et al. (1999) and Gnedin & Ostriker (1997), for the redshifts we consider here. This value of c_L also results in reionization epochs for H I and He II that span ranges

consistent with observations, for the various cases that we consider in § 3.

As an aside, we note that c_L and f_{esc} are inherently related, owing to their strong dependence on the scale on which they are defined. Some numerical simulations of reionization by stars appear to require values of $f_{esc}^H \sim 0.5$–1 (Gnedin 2000; Benson et al. 2002) in order to have the calculated values of $z_{reion,H}$ be consistent with observations. In the case of Gnedin (2000), this seemingly high value of f_{esc}^H is misleading, since it is in fact defined as the value at the surface of the star and does not correspond to the f_{esc}^H relevant for those ionizing photons that reach the IGM, as defined in this work. The loss of ionizing photons within individual halos is compensated through a clumping factor for H II regions that accounts for this, so that at early times, the c_{HII} in Gnedin (2000) exceeds values of a few thousand. For models that define f_{esc}^H at the halo/IGM scale, the appropriate c_{HII} is the one in Gnedin & Ostriker (1997) or Madau et al. (1999) rather than the one in Gnedin (2000). Thus, the recombinations from the stellar surface to the edge of the galactic halo are not double-counted (N. Y. Gnedin 2002, private communication).

To summarize, our adopted standard model (SM) of reionization is parameterized by the currently favored spatially flat cosmology described by the parameter set $[\sigma_8, n, h, \Omega_b, \Omega_\Lambda, \Omega_M, c_L, f_\star, f_{esc}^H, f_{esc}^{He}] = [0.9, 1.0, 0.7, 0.04, 0.7, 0.3, 30, 0.05, 0.05, 0.025]$, where h is the Hubble constant in units of 100 km s^{-1} Mpc^{-1} and Ω_b, Ω_Λ, and Ω_M represent the cosmological density parameters of baryons, the cosmological constant, and matter, respectively. Our reionization model is described by the collapsed baryon fraction F_B and the volume filling factors F_i, where

$$F_B(z) = \text{erfc}\left(\frac{\delta_c}{\sqrt{2}\sigma(R,z)}\right), \quad (1)$$

$$F_i(z) = \rho_B(z) \int_{25}^{z} dz_{on} \frac{dF_B}{dz}(z_{on}) \left[\frac{4\pi}{3} r_{I,i}^3(z_{on}, z, M(z_{on}))\right]. \quad (2)$$

Here i corresponds to H II or He III, the critical overdensity $\delta_c(z)$ equals 1.686 multiplied by a cosmology-dependent growth factor (Eisenstein & Hu 1998), $\rho_B(z)$ is the average IGM baryon density, z_{on} is the source turn-on redshift (we set the earliest redshift at which star formation occurs to be 25), and $\sigma(R,z)$ is evaluated with a spherical top-hat window function over a scale $R \propto M_h$, where $M_h \equiv 10^8 M_\odot[(1+z_{on})/10]^{-1.5}$ is the minimum total halo mass (the sum of DM and baryons) that has collapsed at a source turn-on redshift z_{on} utilizing H-line cooling, and $M \equiv (\Omega_b/\Omega_M)M_h$. We solve numerically for the radius of the I-front $r_{I,i}$, whose evolution as a function of z_{on}, M, z, and the time-dependent stellar ionizing fluxes is described below.

We define reionization as the overlap of individual ionized regions of the relevant species, i.e., when the volume filling factors of ionized hydrogen and helium F_{HII} and F_{HeIII} equal 1. These are roughly equivalent to the volume-averaged ionization fractions of each species if almost all of the baryons are in the IGM up through reionization, which is consistent with numerical simulations of the evolution of structure. We emphasize that the semianalytic treatment here defines reionization as the overlap of fully ionized regions in the IGM and corresponds to the component of the IGM that dominates the ionization by volume filling

factor at high redshift. By this definition, reionization precedes the GP trough's disappearance, which represents the ionization of any remaining H I/He II in overdense portions of the IGM or in individual ionized regions. Put another way, in the terminology of Gnedin (2000), the model here is an accurate description of the "preoverlap" and "overlap" phases of reionization but not of the "postoverlap" epochs, which correspond to the "outside-in" ionization of neutral dense regions. In a strict sense, the volume filling factors of H II and He III can never equal unity exactly owing to the presence of neutral regions in the universe, whose evolution we do not track here, well after the reionization of the IGM. Although we include the effects of IGM clumping in this paper, the development of luminous objects and the gradual overlap of H II regions are themselves characterized only in an average sense. In reality, the first astrophysical sources of ionizing photons are likely to be located in dense regions embedded in the large-scale filamentary structure of matter, so that reionization is a highly nonlinear, inhomogeneous process. To truly probe the complex details of this patchy reionization, one must turn to numerical simulations, which can follow the detailed radiative transfer, perform the necessary characterization of spatial variations, and reveal the full three-dimensional topology of reionization.

In Paper I, we present newly calculated evolving spectra for Population III stars, which can be converted into an ionizing photon rate as a direct input to our reionization model. We reproduce this figure from Paper I here for continuity. In Figure 1, we display the evolving spectra for continuous and instantaneous star formation for synthetic clusters of Population III stars, as well as for a representative example of Population II stars corresponding to stellar metallicities $Z = 0.001$ (Leitherer et al. 1999). The instantaneous case converts $10^6 M_\odot$ into stars in a burst at time $t = 0$; in the continuous case, gas is converted into stars at the steady rate of 1 $M_\odot$ yr^{-1}. The composite spectra (excluding nebular emission) are shown at times of 1 and 15 Myr. We assume that the stars form in a Salpeter IMF from 1 to 100 $M_\odot$, which is reasonable in the absence of a complete theory of primordial star formation.

Figure 1 also shows the H I and He II ionizing photon production rates Q_0 and Q_2, respectively, for these synthetic clusters. For the Population II case, we plot the cluster Q_2 when Wolf-Rayet stars are included and excluded. This provides an indication of the role played by stellar mass loss in the gain in He II ionization from Population II to Population III. This gain could be lowered if there were significant numbers of Wolf-Rayet stars at Population II metallicities. As we discuss in Paper I, the presence of the Wolf-Rayet phenomenon at high redshift and low metallicity is thought to be unlikely. We therefore focus in this paper on directly comparing the ionizing radiation from the main-sequence phases of Populations II and III; this roughly brackets the range of their effects on reionization, particularly for He II. From Figure 1, the Population III cluster has 60% stronger H I ionization and 10^5 times more He II ionizing photons relative to the Population II cluster with the same IMF and total mass, excluding Wolf-Rayet stars. These differences, particularly for He II, could have potentially large effects for the reionization of the IGM, which we examine in § 3. Also displayed in the top right panel of Figure 1 are the instantaneous values of Q_2 from the ZAMS corresponding to stellar carbon abundances $Z_C = 10^{-8}$, 10^{-7}, and 10^{-6}, marked with filled squares. These are intended to mimic the effects
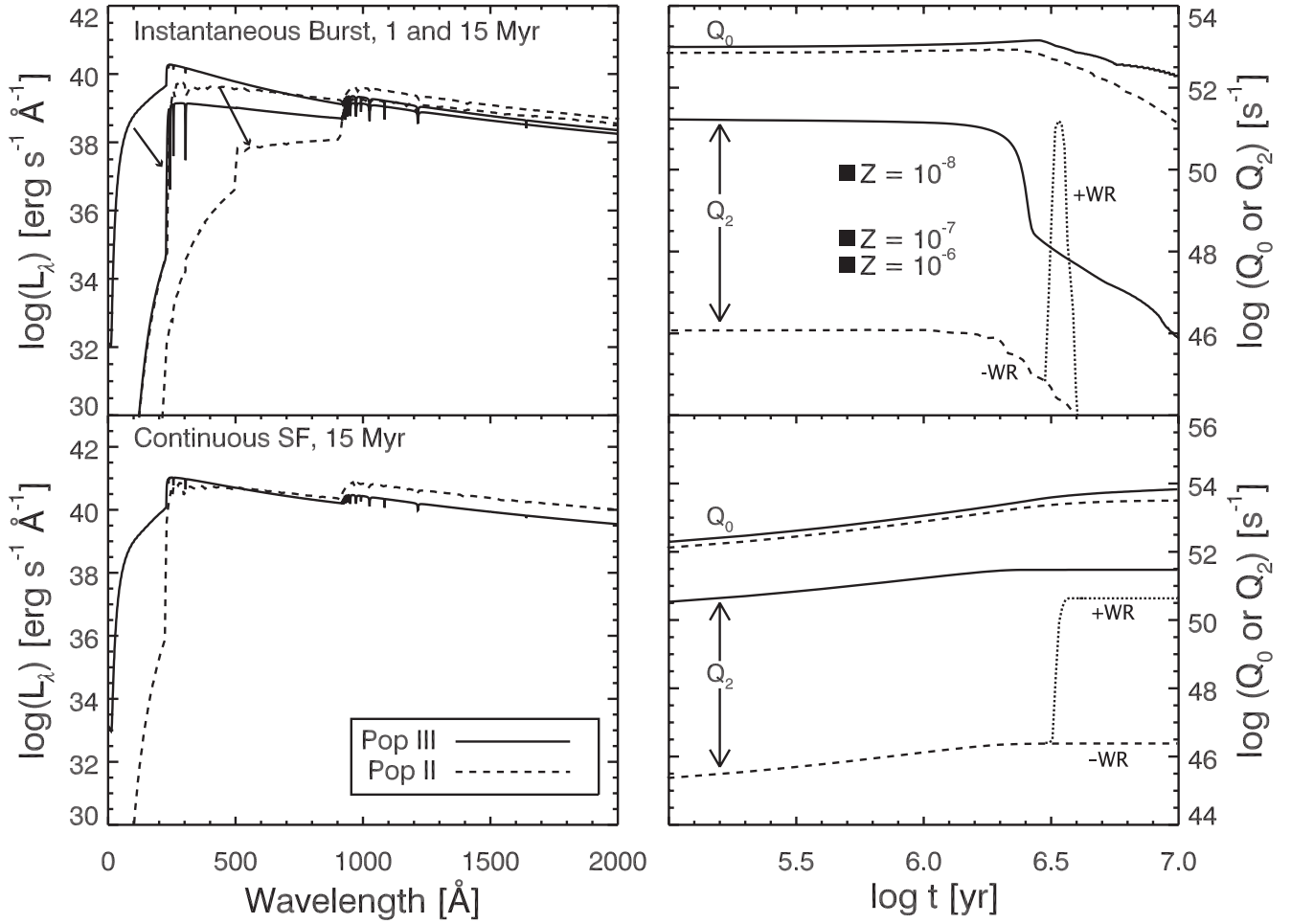
FIG. 1.—Comparison of evolving spectra Q_0 and Q_2 for synthetic Population II and Population III stellar clusters. *Top left*: Composite spectra for Population II (*dashed lines*) and Population III (*solid lines*) clusters at times of 1 and 15 Myr after converting $10^6 \, M_\odot$ into stars in a Salpeter IMF from 1 to 100 $M_\odot$ in an instantaneous burst. At 15 Myr the Population II spectrum has faded in H I ionization, but the Population III cluster is still a significant source of H I ionization, owing to the presence of $Z = 0$ stars with $M = 10$–$15 \, M_\odot$ and $T_{\rm eff} > 50{,}000$ K. No nebular emission is included here. *Bottom left*: Example spectra for the continuous star formation case at 15 Myr, which forms stars in a Salpeter IMF from 1 to 100 $M_\odot$ at the rate of 1 $M_\odot$ yr^{-1}. *Top and bottom right*: IMF-weighted cluster Q_0 and Q_2 corresponding to the instantaneous/continuous cases at left. For Population II, the cluster Q_2 is plotted for the cases when Wolf-Rayet stars are included (*dotted lines*) and excluded (*dashed lines*), indicating the effects of stellar mass loss on the gain in He II ionization from Population II to Population III. In the top right panel we mark with filled squares the instantaneous values of Q_2 from the ZAMSs with carbon abundances $Z_C = 10^{-8}$, 10^{-7}, and 10^{-6}. These points show the sharp decline in He II ionizing photon production when small abundances of ^{12}C are included.

of trace levels of ^{12}C in the stellar core and to represent a possible "second generation" of stars. These points show the sharp decline in the He II ionizing photon production when small abundances of ^{12}C are available to stars.

We provide here the fits[6] for the logarithms of the ionizing photon rates, $\log(Q_0)$ and $\log(Q_2)$, of a $10^6 \, M_\odot$ Population III cluster in the instantaneous burst case (see § 3 for the continuous star formation case); these are good to within a few percent over the fitted range. The time variable is $T \equiv \log t$, where t is the time in years since the cluster turned on. For $t = 0$–2.8 Myr,

$$\log(Q_0) = 54.16 - 0.5T + 0.053T^2 \; ; \qquad (3)$$

---

for $t = 2.8$–30 Myr,

$$
\begin{aligned}
\log(Q_0) = &-128.24 + 175.1T - 17.92(3T^2 - 1) \\
&+ 1.35(5T^3 - 3T) - 0.0086(35T^4 - 30T^2 + 3) \\
&- 0.21 \exp[-0.5(T - 7.22)^2] \; .
\end{aligned} \qquad (4)
$$

After this time, Q_0 drops to about 1% of its value at $t = 0$, and we set $Q_0 = 0$ for convenience, although this is not strictly true. For He II, from $t = 0$–0.9 Myr,

$$\log(Q_2) = 50.72 + 0.235T - 0.027T^2 \; ; \qquad (5)$$

for $t = 0.9$–2.55 Myr,

$$
\begin{aligned}
\log(Q_2) = &-\exp[31.33(T - 6.44)] \\
&\times (-0.047T + 5.13) - \frac{(T - 6.08)^2}{0.43} + 0.77 \; ,
\end{aligned} \qquad (6)
$$

and we set $Q_2 = 0$ after 2.55 Myr.

---

[6] We refer the reader to Schaerer (2002) for a detailed treatment and fits of the time-averaged ionizing photon rates as a function of stellar mass for $Z = 0$ stars. The IMF-averaged ionizing fluxes provided there as a function of time are in agreement with our results here.

The growth of individual ionized regions is a function of the time-dependent source luminosity and the stellar cluster's turn-on redshift, and their evolution is given by the balance between photoionization and recombination in an expanding IGM (Shapiro & Giroux 1987; Donahue & Shull 1987). The differential equations describing the evolution of the I-fronts' radii for H II and He III, $r_{I,H}(t)$ and $r_{I,He}(t)$, in equation (2) are

$$n_H(t)\left[\frac{dr_{I,H}}{dt} - H(t)r_{I,H}\right] = \frac{1}{4\pi r_{I,H}^2}$$
$$\times \left[f_* f_{esc}^H Q_0(t) - \frac{4\pi}{3}\alpha_{H I}^B c_L n_e(t) n_{H II}(t) r_{I,H}^3\right], \quad (7)$$

$$n_{He}(t)\left[\frac{dr_{I,He}}{dt} - H(t)r_{I,He}\right] = \frac{1}{4\pi r_{I,He}^2}$$
$$\times \left[f_* f_{esc}^{He} Q_2(t) - \frac{4\pi}{3}\alpha_{He II}^B c_L n_e(t) n_{He III}(t) r_{I,He}^3\right].$$
$$(8)$$

We assume case B recombination for both H II and He III in the pre-reionization IGM, since the Lyα and recombination-line photons for both of these are likely to be resonantly scattered and absorbed locally. The line and continuum recombination photons to the $n = 1$ states, if sufficiently redshifted, could potentially be relevant for the global radiation field at subsequent epochs, especially for case B recombination. This is unlikely, however, to be a large effect prior to the full reionization of the IGM. A realistic description of recombination will lie somewhere between case A and case B. We proceed here with the assumption of case B recombination and reduce the above equations to

$$\frac{dr_{I,H}^3(t)}{dt} = 3H(t)r_{I,H}^3(t) + \frac{3}{4\pi n_H(t)}$$
$$\times \left[f_* f_{esc}^H Q_0(t) - \frac{4\pi}{3}r_{I,H}^3 \alpha_{H I}^B c_L n_e(t) n_{H II}(t)\right], \quad (9)$$

$$\frac{dr_{I,He}^3(t)}{dt} = 3H(t)r_{I,He}^3(t) + \frac{3}{4\pi n_{He}(t)}$$
$$\times \left[f_* f_{esc}^{He} Q_2(t) - \frac{4\pi}{3}r_{I,He}^3 \alpha_{He II}^B c_L n_e(t) n_{He III}(t)\right].$$
$$(10)$$

At each redshift, we solve numerically for the growth of the I-fronts with a fourth-order Runge-Kutta method for all the preceding source turn-on redshifts, each corresponding to $t = 0$ in equations (9) and (10). The time steps at each redshift are set to be 5%–10% of the recombination timescale appropriate for H II or He III at that redshift. These were the largest time steps that ensured numerical convergence of the results. The recombination timescale is given by

$$\bar{t}_{rec}(z) = \frac{1}{\alpha^B c_L(1 + 2x_{He})\bar{n}_H(z)}, \quad (11)$$

where $\bar{n}_H(z)$ is the average total number density of hydrogen in the IGM [$\bar{n}_H(z=0) \sim 1.7 \times 10^{-7}$ cm^{-3} in our SM], x_{He} is the ratio of He to H by number, about 0.0789 for $Y_{He} = 0.24$, $n_e = n_{H II} + 2n_{He III} = (1 + 2x_{He})n_H$, under the assumption that all H or He in the vicinity of the I-front is in

the form of H II or He III, respectively, and α^B is the case B recombination coefficient for H II or He III. By virtue of the definition of c_L, equation (11) assumes a spatially constant α^B. Furthermore, since we do not solve in detail for the thermal evolution of the IGM in the vicinity of the I-fronts, we assume a temperature of 10^4 K and take $\alpha_{H I}^B(10^4$ K$) = 2.59 \times 10^{-13}$ cm^3 s^{-1}, with $\alpha_{He II}^B(10^4$ K$) = 5.83\alpha_{H I}^B(10^4$ K$)$ (Spitzer 1978).

This method of solving for the nonequilibrium growth of the I-fronts of H II and He III is a significant improvement on the treatment in V2000, which used the analytic solutions for $r_{I,i}(t)$ provided by Shapiro & Giroux (1987). The drawback of that method was the underlying assumption of a constant source luminosity. In the present treatment, the evolution of the I-fronts is followed more accurately, and we can distinguish between the cases of continuous and bursty star formation.

3. RESULTS

In this section, we focus on the effects of the first stars on cosmological reionization, using the model described in § 2. Specifically, we consider combinations of evolving Population III and Population II spectra in continuous and bursty star formation scenarios, whose definitions directly correspond to those in Figure 1. In the case of continuous star formation, we take the appropriate values of Q_0 and Q_2 for Population III or II at a time of 10^6 yr from Figure 1, when the cluster stellar masses equal 10^6 $M_\odot$. We do this to be consistent with the case of synthetic spectra for a burst of star formation for a 10^6 $M_\odot$ cluster: the star formation rate for the continuous case being 1 $M_\odot$ yr^{-1}, the total gas mass converted to stars equals that for bursty star formation at a time of 1 Myr. For Population III, $Q_0 = 1.04 \times 10^{53}$ s^{-1} and $Q_2 = 1.56 \times 10^{51}$ s^{-1}. For the adopted Population II cluster, $Q_0 = 7.76 \times 10^{52}$ s^{-1} and $Q_2 = 1.32 \times 10^{46}$ s^{-1}.

The cases considered below are intended to provide an indicative range for the effects of Population III stars on the reionization of the high-z IGM, given reasonable values for the many parameters that describe the model. As emphasized earlier, the issues of the sources of reionization and the formation sites and cosmological significance of the first (presumably metal-free) stars are at present unresolved. Furthermore, the nature of high-z star formation is completely unknown and may not separate cleanly into bursty versus continuous modes. Thus, the distinction drawn below between Populations III and II is convenient rather than exact, owing to the lack of detailed evolving spectra in the literature for stellar metallicities between ~0.001 and 0 (Schaerer 2002 has computed the case of $Z = 0.0004$ stars, albeit with mass loss and for a different range of the stellar IMF than we consider here). We present the results below with the understanding that reality lies somewhere between the considered cases.

3.1. Pure Population III Stellar Spectra

We begin by considering the extreme case in which Population III stellar spectra are assumed for all star formation through reionization. This is clearly not realistic; the reader may take the results here to represent the most extreme effects of metal-free stars. In Figure 2, we display the redshift evolution of F_B, $F_{H II}$, and $F_{He III}$ for the SM with continuous and bursty star formation with evolving Population
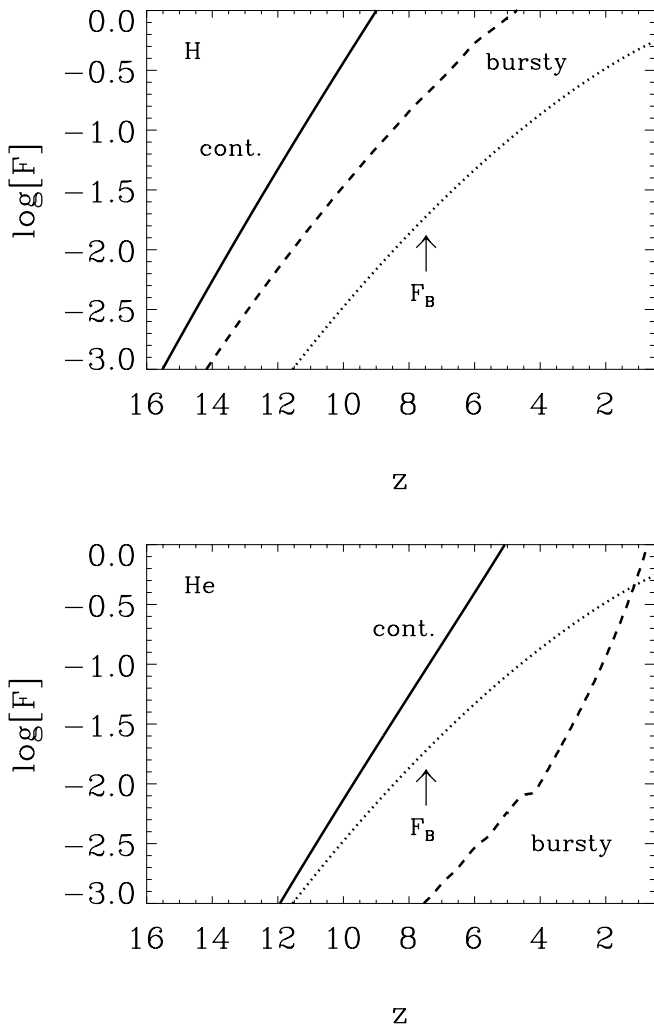
FIG. 2.—Redshift evolution of the fraction of baryons in star-forming halos, F_B (*dotted lines*), and the volume filling factors of H II and He III, $F_{H II}$ and $F_{He III}$, for the standard model in this work: $\sigma_8 = 0.9$, $\Omega_b = 0.04$, $h = 0.7$, $n = 1.0$, $\Omega_\Lambda = 0.7$, $\Omega_M = 0.3$, $c_L = 30$, $f_* = 0.05$, $f_{esc}^H = 0.05$, and $f_{esc}^{He} = 0.025$. Top and bottom panels display $F_{H II}$ and $F_{He III}$, with solid and dashed lines in each panel representing continuous and bursty star formation, respectively, with evolving Population III spectra.

III spectra. We do not display the evolution of $F_{H II}$ and $F_{He III}$ here or in subsequent figures after these quantities equal unity, since the model in this work describes reionization accurately only up through the overlap stage. The values of these three quantities are also shown in Table 1 at a series of sample redshifts, for the various cases depicted in Figure 2.

For continuous or bursty Population III star formation, H I reionization[7] occurs at $z \sim 9$ or 4.7 and that of He II at $z \sim 5.1$ or 0.7, respectively. As may be expected, reionization occurs later for both H I and He II in the case of evolv-

ing spectra from an instantaneous burst relative to those from the continuous case. This can be attributed to the decline in ionizing photons at times exceeding a few million years as the burst fades. A critical question, which we have sidestepped here, is what determines the time lag between bursts of star formation at early epochs. Clearly, in the limit of zero lag, there will be no distinction between continuous and bursty modes, as far as the emergent spectra for the IGM are concerned. Since this issue is unresolved, Figure 2 shows the range of the effects of Population III stars alone on reionization for both star formation modes. For both H I and He II, this range contains the current observational values of their respective reionization epochs, $z_{reion,H} \sim 6$ and $z_{reion,He} \sim 3$.

3.2. *Population III Switching to Population II*

A more realistic description of the role played by stars in reionization should involve stellar populations of nonzero metallicity in addition to Population III. This translates into solving the problem of the complex interplay between cosmological metal transport and the mixing timescales in the ISM of individual high-z halos, in which the metals generated by the first population of stars are incorporated into subsequent stellar generations. This is, however, likely to be influenced heavily by the local balance between stellar/SN feedback and the availability of coolants, a problem whose inherent dependence on spatial inhomogeneity places it beyond the scope of this work. We attempt below to evaluate the effect of Population III ($Z = 0$) stars, which then switch to Population II ($Z = 0.001$) stars at some later time, with the caveat that this definition of Population II is one based on the available spectral templates of nonzero metallicity. We stress that the transition from Population III to Population II is driven by the physical condition of a metallicity threshold rather than a fixed timescale for halo self-enrichment. In reality, Population II star formation may span a range of metallicities between $Z = 0$ and $Z = 0.001$, corresponding to many generations of stars. The transition from Population III to Population II may occur at, e.g., a metallicity of 10^{-4} $Z_\odot$, as some authors have found (Schneider et al. 2002 and references therein). For our purposes below, the important distinction is between stellar populations that generate He II ionizing photons and those that do not. This rough division is justified by the steep dependence of Q_2 on the stellar metallicity (Fig. 1).

An estimate of the time at which Population III star formation ceases and that of Population II begins involves assumptions about many physical processes that are not yet well understood, such as the mixing and reincorporation timescales for the generated metals. We consider only continuous star formation, because for bursts it becomes difficult to define an average global time when Population II star formation begins. Moreover, pockets of metal-free gas cannot be ruled out at any epoch. In addition, the nature of the Press-Schechter method complicates the treatment of bursty star formation. The formalism is designed to track which mass overdensities are going nonlinear at any redshift, but it does not have information on the detailed stellar history of the baryons in halos at those epochs. Thus, for an individual halo, the connection between the time elapsed from the onset of Population III star formation and the age of the universe is made more consistently for continuous rather than bursting modes. This would correspond to a

---

[7] Although we do not include low-mass halos in this work for the reasons detailed in § 2, the details of the radiative feedback on early star-forming halos are not yet quantitatively resolved. As a comparison with the results in this section, we find that the general effect of including halos with virial temperature above 10^3 K (rather than 10^4 K) is an increased reionization redshift. Specifically, for continuous or bursty Population III star formation, H I reionization occurs at $z \sim 11.8$ or 6.2 and that of He II at $z \sim 6.3$ or 0.7, respectively.

TABLE 1
EVOLUTION OF BARYONS IN HALOS AND IGM IONIZATION FRACTIONS

		$F_{\mathrm{H\,II}}$				$F_{\mathrm{He\,III}}$			
				Pop. III/II				Pop. III/II	
z	F_B	Pop. III (Bursty)	Pop. III (Continuous)	10^8 yr	10^9 yr	Pop. III (Bursty)	Pop. III (Continuous)	10^8 yr	10^9 yr
20.........	2.7E−7	2.1E−6	4.4E−6	3.3E−6	4.4E−6	1.3E−8	8.5E−8	7.2E−13	8.5E−8
15.........	4.9E−5	4.6E−4	1.8E−3	1.3E−3	1.8E−3	2.5E−6	3.5E−5	3.0E−10	3.5E−5
10.........	3.3E−3	3.4E−2	0.37	0.27	0.37	1.7E−4	7.4E−3	6.2E−8	7.4E−3
9............	6.8E−3	7.1E−2	~1	0.74	~1	3.6E−4	0.02	1.7E−7	0.02
7............	2.6E−2	0.27	~1	~1	~1	1.6E−3	0.15	1.2E−6	0.15
6............	4.7E−2	0.53	~1	~1	~1	2.9E−3	0.39	3.3E−6	0.39
4............	0.13	~1	~1	~1	~1	1.0E−2	~1	2.6E−5	2.6E−5
3............	0.22	~1	~1	~1	~1	3.2E−2	~1	7.9E−5	7.9E−5
2............	0.33	~1	~1	~1	~1	0.12	~1	2.8E−4	2.8E−4
0............	0.62	~1	~1	~1	~1	~1	~1	8.9E−3	8.9E−3
z_{reion}		4.7	9	8.7	9	0.7	5.1	...	...

NOTES.—This is the redshift evolution of the collapsed baryon fraction F_B and the volume filling factors $F_{\mathrm{H\,II}}$ and $F_{\mathrm{He\,III}}$ (or equivalently, the volume-averaged IGM H II and He III ionization fractions) for the four standard model scenarios (see text) displayed in Figs. 2–3, with star formation beginning at $z = 25$. For the cases in the last two columns, He II never reionizes completely but reaches a maximum ionization fraction of ~8.9E−3 at $z \sim 0$ or 0.6 at $z \sim 5.6$ for a duration of Population III star formation of 10^8 or 10^9 yr.

"universal" self-enrichment timescale. This timescale could be increased by the preferential ejection of metals into the IGM through SN feedback or decreased if the metals cool rapidly and exist predominantly in a cold ISM phase rather than a hot phase. Given these uncertainties associated with the incorporation of freshly synthesized metals into new stars, we consider two ISM mixing timescales that span an order of magnitude, 10^8 and 10^9 yr (de Avillez & Mac Low 2002).

In Figure 3 we display the redshift evolution of $F_{\mathrm{H\,II}}$ and $F_{\mathrm{He\,III}}$ for the cases of Population III stars lasting for 10^8 and 10^9 yr, after which the ionizing spectra switch to Population II. As in § 3.1, the values of these quantities are shown in Table 1 at a series of redshifts for the SM cases depicted in Figure 3. In addition, we show a case for $F_{\mathrm{He\,III}}$ in which Population III spectra switch to Population II at 10^9 yr, with $c_L = 30$ for times up through 10^9 yr and $c_L = 1$ at times exceeding 10^9 yr. We do this in order to provide an indication of the fate of those IGM regions that are not strongly clumped, after they have experienced partial ionization from early Population III stellar activity. Such regions, with overdensities of order 1 to a few and $c_L \sim 1$, are likely to be the dominant component of the IGM by volume at late epochs. Their evolution, once the Population III ionizing sources turn off, is dominated by recombinations and is hence sensitive to the chosen value of c_L.

We find that H I reionization occurs at $z \sim 9.0$ or 8.7 for Population III star formation lasting for 10^9 or 10^8 yr. This small difference in the reionization epochs is not surprising, given that the H I ionizing photon rates between Populations III and II differ only by about 60%. In addition, since the age of the universe exceeds 10^9 yr only at $z \lesssim 6$, the case of Population III stars lasting for 10^9 yr is effectively no different from that of considering only Population III spectra (Fig. 2, continuous star formation case).

The duration of Population III activity has, however, more dramatic consequences for He II reionization, given the many orders of magnitude difference between the Population III and Population II He II ionizing fluxes. Although He II never reionizes completely in any of the cases, the sce-

nario with a 10^9 yr Population III timescale reaches ionization fractions of about 60% by $z \sim 5.6$, when Population III stars are turned off. Subsequent to that, the ionization of He III plummets to very low values for $c_L = 30$, effectively to the Population II curve, and recovers mildly by $z \sim 0$. Although the redshift of the precipitous drop in $F_{\mathrm{He\,III}}$ is an artifact of the Population III timescale considered here, the strong decrease in $F_{\mathrm{He\,III}}$ itself is real, since it is tracked over about a hundred time steps over $\Delta z \sim 0.5$. For the case with a 10^9 yr Population III timescale in which $c_L = 30$ up through the He III ionization peak at $z \sim 5.6$ and $c_L = 1$ afterward, recombinations are less effective at $z \lesssim 5.6$. Hence, the He III ionization fraction declines more gradually and remains at levels of about 3% at $z \sim 0$. Together, these two cases provide an indicative range of the evolution of IGM regions that have experienced partial He II ionization by Population III stars in our reionization model.

From the results presented through this point, we see that He II may experience full or partial ionization followed by recombination, depending on the duration of Population III stellar activity, prior to its currently detected reionization epoch of $z \sim 3$. The fate of any ionized "relic" He III regions, particularly in the IGM "voids," is discussed further in § 3.4.

3.3. The Amount of Small-Scale Power

The redshift z_{reion} at which H I or He II reionization occurs is sensitive to the amount of small-scale power available in the structure formation model for the first luminous objects. This epoch is determined primarily by two cosmological parameters, σ_8 and n, which we use as inputs to quantify reionization. An increase in either of these parameters directly leads to enhanced small-scale power and earlier reionization; in particular, z_{reion} is affected strongly by n (see, e.g., Venkatesan 2002) for the case of H I reionization. Thus, even if we assume that all the other parameters characterizing reionization are well constrained, n and σ_8 have to combine in the right way to meet the observational limits on z_{reion}. In this era of precision cosmology, most cosmolog-
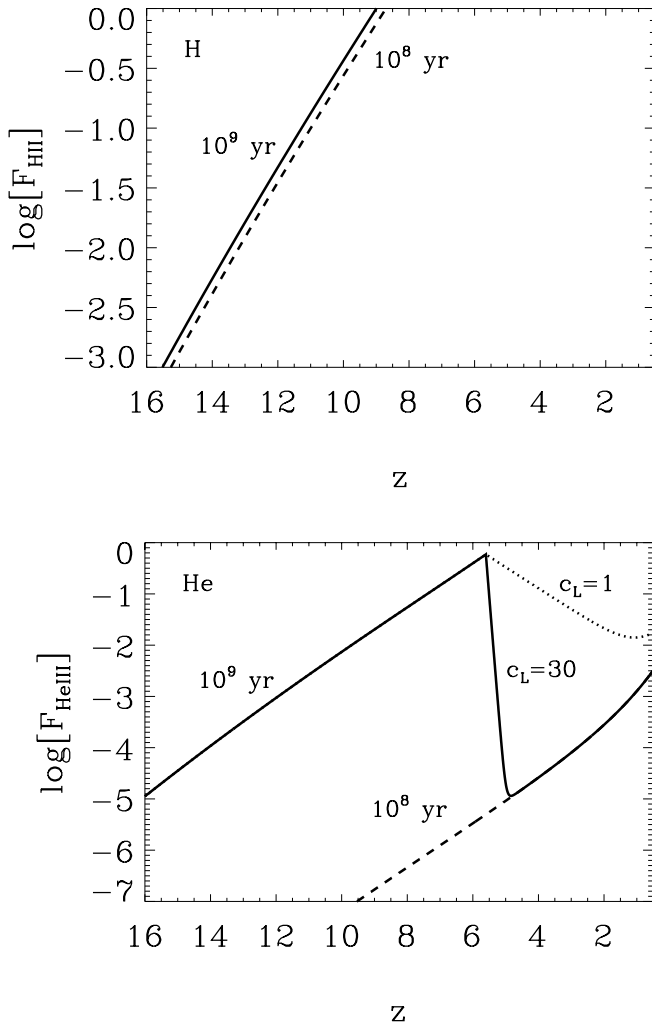
FIG. 3.—Redshift evolution of the volume filling factors of H II, $F_{H II}$, and He III, $F_{He III}$, shown for the standard model in this work. Top and bottom panels display $F_{H II}$ and $F_{He III}$, respectively, for continuous star formation. Solid and dashed lines in each panel represent Population III spectra switching to Population II at times corresponding to ages of the universe of 10^9 and 10^8 yr. For $F_{He III}$, an additional case is shown with a dotted line, where Population III spectra switch to Population II at 10^9 yr with the assumption of a homogeneous IGM ($c_L = 1$) at $z \lesssim 5.6$. This is intended to mimic the fate of low-density regions in the IGM subsequent to partial ionization (see text).

TABLE 2
REIONIZATION EPOCH AND SMALL-SCALE POWER

| | $z_{reion,H}$ FOR $\sigma_8 = 0.7$ ($\sigma_8 = 0.9$) | | |
POPULATION	$n = 0.9$	$n = 1$	$n = 1.1$
Population III (bursty).............	3.5 (4.2)	3.9 (4.7)	4.4 (5.4)
Population III (continuous)	5.9 (7.7*)	7.0* (9.0*)	8.3* (10.6)

NOTES.—These are the redshifts $z_{reion,H}$ of hydrogen reionization for $\sigma_8 = 0.7$ and $\sigma_8 = 0.9$ and for values of n spanning its current range from observations (0.9–1.1). All other parameters are fixed at their standard model values. The two modes of Population III star formation indicate the possible ranges for $z_{reion,H}$ for a given set of parameters; in particular, the continuous star formation case represents the most extreme effects of metal-free stars. The cases that are consistent with current data on $z_{reion,H}$ are marked by asterisks.

reasonable values for the astrophysical parameters in our reionization model.

The current limits on n are about 0.9–1.1 from a combination of data on the CMB, large-scale structure, and the Lyα forest (see, e.g., Wang et al. 2002; Pryke et al. 2002), with a preference in this range for $n \sim 0.9$–1.0 from analyses of joint data sets. In Table 2, we show the values of $z_{reion,H}$ for $\sigma_8 = 0.7$ and $n = 0.9$, 1.0, and 1.1, for the two cases of continuous and bursty Population III star formation. The corresponding numbers for $\sigma_8 = 0.9$ are shown in parentheses for each case. As emphasized earlier, the case of continuous star formation is intended to demonstrate the most extreme effects of $Z = 0$ stars. The bursty case provides a lower limit to $z_{reion,H}$ here, but its inherent dependence on the unknown time lag between bursts implies that even lower values of $z_{reion,H}$ are possible.

When we compare the values of $z_{reion,H}$ from Table 2 with current data, the following cases appear to be inconsistent with observations, within the uncertainties of our reionization model: $0.9 \leq n \leq 1.1$ with $\sigma_8 = 0.7$ or $\sigma_8 = 0.9$ (bursty case), $n = 0.9$ with $\sigma_8 = 0.7$ (continuous case), and $n = 1.1$ with $\sigma_8 = 0.9$ (continuous case). Those of the excluded cases with $n = 0.9$ are worth noting, since this value for n is preferred by the most recent joint data set analyses such as Wang et al. (2002) and Tegmark, Zaldarriaga, & Hamilton (2001). Note that we treat reionization through the overlap phase, but not the " clearing out " of the last dense neutral regions in the IGM. Thus, the numbers in Table 2 are, in this sense, an upper bound to the redshift of reionization as determined by GP troughs. A more detailed treatment using numerical simulations would result in a slightly downward revision of $z_{reion,H}$ in Table 2.

We emphasize that the relation between n, σ_8, and $z_{reion,H}$ as shown in Table 2 is oversimplified, given the uncertainties in our reionization model. These include the unknown parameters quantifying Population III star formation (such as the IMF, mode of star formation, and the maximum stellar masses in the IMF). In addition, the matter power spectrum may not be described on all scales by a single value of n, and the feedback from stars and SNe on baryons in halos could partially erase the correlation between small-scale power and $z_{reion,H}$. Alternatively, $z_{reion,H}$ could be raised by increasing f_* or f_{esc}^H in the model. This would require star formation to be more efficient and/or more widespread than we have assumed in the SM or would require the escape fraction of ionizing radiation to be larger. This is something that observations of the local universe do not

ical parameters are becoming highly constrained, with σ_8 remaining as one of the few parameters with significant uncertainty. As noted earlier, the data on σ_8 appear to be divided into two values, a high value of about 0.9–1.0 (Evrard et al. 2002; Zhang, Pen, & Wang 2002; Refregier et al. 2002) and a low value of about 0.7 (Reiprich & Böhringer 2002; Seljak 2002), each with a claimed error bar of about 10%. In this section, we examine the consequences of a low value for σ_8 for $z_{reion,H}$ (we chose $\sigma_8 = 0.9$ for our SM), given the current uncertainty in the value of n. We focus on H I in particular, since the detection of $z_{reion,H}$ is the next observational frontier of interest for reionization. This quantity can potentially be a useful probe of the small-scale power in a reionization model. We emphasize that we are not assuming that the astrophysics of reionization is completely understood. Rather, we are interested in the consequences of lowering the value of σ_8 for reionization, given

support, although we cannot rule this out. Our main point here is that the relation between n, σ_8, and $z_{reion,H}$, subject to the above caveats, can be useful if combined with future observational determinations of $z_{reion,H}$ and even slightly tighter limits on n. In particular, this technique potentially has the power to rule out the combination of low values of $\sigma_8 \lesssim 0.7$ and $n < 1$.

3.4. *The Fate of Primordial* He III *Regions*

The possibility of an early epoch of partial He II reionization in the IGM by Population III stars begs the question of what happens to these regions once the Population III epoch ends. If we can predict the evolution of these early He III regions, we can compare them with the best available constraints on He II ionization in the high-redshift IGM (Kriss et al. 2001; J. M. Shull et al. 2003, in preparation). If the He II in the IGM is reionized shortly after H I reionization is accomplished, will these He III regions recombine by $z \sim 3$, where we have observational constraints?

In a clumpy IGM, we can write the recombination time for He III as a function of the local overdensity δ, where $\delta = n_H / \langle n_H \rangle$, and $\langle n_H \rangle$ is the average total hydrogen density in the IGM. We take a critical mass density $\rho_{crit} = 1.878 \times 10^{-29} h^2$ g cm^{-3} and a primordial He mass fraction $Y = 0.24$ to calculate $\langle n_H \rangle$. Thus,

$$ n_H(z) = (1.71 \times 10^{-7} \text{ cm}^{-3})(1+z)^3 \left(\frac{\Omega_b h^2}{0.02} \right) \delta . \quad (12) $$

The recombination time t_{rec} of He III to He II is given by $t_{rec} = (n_e \alpha_{He II})^{-1}$, where the case B recombination coefficient for He II can be written with an explicit temperature dependence, $\alpha_{He II}^B = 1.51 \times 10^{-12} (T/10^4 \text{ K})^{-0.7}$ cm^3 s^{-1}. Combining these relationships and taking $n_e = 1.16 n_H$ for fully ionized gas with He/H $= 0.0789$ by number, we derive the local recombination time as a function of redshift and overdensity:[8]

$$ t_{rec} = (1.31 \times 10^8 \text{ yr}) \left(\frac{1+z}{10} \right)^{-3} \left(\frac{\Omega_b h^2}{0.02} \right)^{-1} \left(\frac{T}{10^4 \text{ K}} \right)^{0.7} \delta^{-1} . \quad (13) $$

In Figure 4 we plot the values of 4 times this expression and compare them to the time from the reionization of He II to $z = 3$, where we have observational constraints on the ionization of He in the IGM. We choose to display $4 t_{rec}$ in order to indicate a recombination e-folding timescale over which the evolving IGM ionization fraction changes appreciably ($e^{-4} \sim 0.02$, whereas $e^{-1} \sim 0.37$). We have explored the possibility that the He II in the IGM was first reionized to He III at $z \sim 5$ by zero-metallicity stars. Figure 4 shows that the void regions with $\delta \lesssim 0.3$ would not have time to recombine before $z = 3$. Such relic He III regions may be visible to sensitive observations of the He II GP effect. However, the large numbers of quasars being discovered at redshifts $z \geq 4$ (Fan

FIG. 4.—Comparison of 4 times the He III to He II recombination time (*e*-folding timescale; see text) for four values of overdensity δ in the IGM with the elapsed time from redshift z to $z = 3$, as a function of redshift. For $\delta \lesssim 1.0$, the recombination time is longer than the time to $z = 3$ and the Hubble time. These regions do not have time to recombine before $z = 3$, where we have observational constraints. We have neglected the photoionization from high-redshift quasars, whose effects could be significant at $3 < z < 6$.

et al. 2001) are likely to provide sufficient ionizing radiation to affect the He II ionization fraction, $f_{He II} = n(\text{He II})/n(\text{He})$. Because $f_{He II} \ll 1$, a small fraction of He III recombinations, together with photoionization by QSO radiation, can shift the He II ionization and the He II/H I ratio η. The detailed ionization history would require a careful integration of the nonequilibrium H I and He II chemistry, which is beyond the scope of this paper.

Fardal, Giroux, & Shull (1998; see also Miralda-Escudé & Ostriker 1992) define the He II to H I column density ratio to be

$$ \eta \equiv \frac{n_{He III}}{n_{H II}} \frac{\alpha_{He II}}{\alpha_{H I}} \frac{\Gamma_{H I}}{\Gamma_{He II}} . \quad (14) $$

This ratio is sensitive to the shape of the ionizing spectrum. Paper I derives the intrinsic η of metal-free stars and the low-metallicity ZAMS. We find that $\eta = 10$ for the Population III ZAMS cluster and remains below 50 for 2.5 Myr. By comparison, $\eta = 20$ for a composite QSO with power-law spectral index $\alpha = 1.8$ (Telfer et al. 2002), and $\eta = 10$ for $\alpha = 1.3$. The low η for the Population III cluster results from its unusual spectrum. The H I photoionization rate $\Gamma_{H I}$ is proportional to the integral above 1 ryd of the specific photon flux times the ionization cross section ($F_\nu \sigma_\nu / h\nu$). For the power-law spectrum, F_ν attains a maximum at 1 ryd, where the cross section peaks. The Population III composite spectrum peaks near 3–4 ryd, where the H cross section is $\sim$64 times smaller (for $\sigma_\nu \propto \nu^{-3}$). We obtain a lower H I photoionization rate for the Population III spectrum and,

---

[8] Gnedin & Ostriker (1997) and Madau (1998) define a spatially averaged recombination time in terms of a clumping factor $C_{H II} = \langle n_{H II}^2 \rangle / \langle n_{H II} \rangle^2$. Their formalism does not follow the recombination of the IGM at a point with a single overdensity. We are interested here in distinguishing between the "filaments" with high δ and "voids" with low δ in observations where the local overdensity is mapped by the Lyα forest. Thus, we define the recombination time here in terms of the local overdensity rather than a spatially averaged clumping factor.

when taken together with its strong He II ionization, a correspondingly lower η.

In a study of the He II GP effect toward HE 2347−4342 with the *Far Ultraviolet Spectroscopic Explorer* (*FUSE*) at $z = 2.3$–2.9, Kriss et al. (2001) found several regions of unusually low η, a signature of hard ionizing sources. Many of these regions can be explained by the contemporaneous presence of QSOs with hard power-law spectra (Telfer et al. 2002; Kriss et al. 2001). In a more detailed analysis of the *FUSE* data, J. M. Shull et al. (2003, in preparation) also find that in void regions with $\log N(\mathrm{H\,I}) < 12.3$, η is systematically higher than 100. These regions can be explained by the presence of more broadly distributed soft sources, such as dwarf galaxies, although this does not explain the large fluctuations in $\eta(z)$. In this picture, the hard sources responsible for low η (QSOs) lie primarily in regions of high neutral hydrogen abundance.

The early He II reionization scenario provides an alternative explanation for the high-η regions. If He is ionized to He III at $z \sim 6$, regions with $\delta > 1.0$ will recombine by $z = 3$, erasing all signatures of the first ionization. However, in the underdense regions with $\delta < 1.0$, there will be time for only partial recombination of He III to He II. These relic He III regions may be detected by sensitive observations of the He II GP effect at high redshift. We note, however, that the rise in the large bright QSO population at $z \lesssim 6$, which we have not accounted for here, will influence the ionization equilibrium of He II and H I in such relic regions. It would then become more challenging to detect this potential signature of metal-free stellar activity. Tests of this idea must await efforts with the *Cosmic Origins Spectrograph* on the *Hubble Space Telescope* to push observations of the He II GP effect to $z > 3$.

4. CONCLUSIONS

We show in Paper I that Population III stars have unusually hard spectra and elevated H I and He II ionizing photon rates. These properties motivated this work, where we examined the role played by these objects in H I and He II reionization through a semianalytic reionization model described by a reasonable set of parameters in the currently favored cosmology. Our general conclusions are as follows:

1. We find that Population III stars can be cosmologically significant for reionization, particularly for He II. For Population III alone, H I and He II reionize at redshifts of $z_{\mathrm{reion,H}} \sim 9.0$ and 4.7 and $z_{\mathrm{reion,He}} \sim 5.1$ and 0.7 for continuous and bursty modes of star formation, respectively.

2. We also considered a more realistic scenario involving a Population III phase of (continuous) star formation that switches to Population II after a self-enrichment timescale for primordial star-forming gas. We find that H I reionization occurs at $z_{\mathrm{reion,H}} \sim 8.7$ or 9.0, depending on whether the Population III stage lasts 10^8 or 10^9 yr. He II never reionizes completely in either case, although the ionization fraction of He III reaches a maximum of about 60% at $z \sim 5.6$ for a 10^9 yr self-enrichment timescale.

3. Since the reionization epoch is sensitive to the power available on small scales, data on H I reionization can critically test, and possibly rule out, low values of σ_8 ($\lesssim 0.7$), particularly if $n < 1$.

By measuring $z_{\mathrm{reion,H}}$ from the CMB and high-z spectroscopic studies and by using direct imaging techniques to detect Population III stellar clusters (Paper I), one can strongly constrain the role played by Population III stars in H I reionization. The current evidence for a complete H I GP trough, and hence $z_{\mathrm{reion,H}}$, comes from the spectrum of a single $z = 6.28$ QSO. The acquisition of more GP data along more lines of sight to sources at $z \sim 6$–9 is required to adequately represent how the appearance and duration of the GP trough varies with redshift. Such observations are within the capabilities of the Sloan Digital Sky Survey, which should detect about 20 bright quasars at $z \gtrsim 6$ during the course of the survey (Becker et al. 2001), and are important targets in the planning of the *James Webb Space Telescope*.

The significance of Population III stars for He II reionization can be tested by future measurements of the He II GP effect in the IGM at $z \sim 3$–5, particularly in underdense regions of the IGM, which may not have had the time to recombine by $z \sim 3$ after experiencing ionization by Population III stars at early times. These relic ionized voids may retain the unique spectral imprint of the first, metal-free stellar populations.

REFERENCES

Abel, T., Bryan, G. L., & Norman, M. L. 2000, ApJ, 540, 39
Abia, C., Domínguez, I., Straniero, O., Limongi, M., Chieffi, A., & Isern, J. 2001, ApJ, 557, 126
Alcock, C., Allsman, R. A., Alves, D. R., Axelrod, T. S., Becker, A. C., & Bennett, D. P. 2000, ApJ, 542, 281
Becker, R. H., et al. 2001, AJ, 122, 2850
Benson, A. J., Lacey, C. G., Baugh, C. M., Cole, S., & Frenk, C. S. 2002, MNRAS, 333, 156
Bromm, V., Kudritzki, R. P., & Loeb, A. 2001, ApJ, 552, 464
Carr, B. J., Bond, J. R., & Arnett, W. D. 1984, ApJ, 277, 445
Cen, R., & Ostriker, J. P. 1993, ApJ, 417, 404
Ciardi, B., Ferrara, A., Governato, F., & Jenkins, A. 2000, MNRAS, 314, 611
Cojazzi, P., Bressan, A., Lucchin, F., Pantano, O., & Chavez, M. 2000, MNRAS, 315, L51
de Avillez, M. A., & Mac Low, M.-M. 2002, in Proc. XVIIth IAP Colloquium, Gaseous Matter in Galaxies and Intergalactic Space, ed. R. Ferlet, M. Lemoine, J.-M. Desert, & B. Raban (Paris: Editions Frontières), 141
Deharveng, J.-M., Buat, V., Le Brun, V., Milliard, B., Kunth, D., Shull, J. M., & Gry, C. 2001, A&A, 375, 805

Dey, A., Spinrad, H., Stern, D., Graham, J. R., & Chaffee, F. H. 1998, ApJ, 498, L93
Donahue, M., & Shull, J. M. 1987, ApJ, 323, L13
Dove, J. B., Shull, J. M., & Ferrara, A. 2000, ApJ, 531, 846
Eisenstein, D. J., & Hu, W. 1998, ApJ, 496, 605
Evrard, A. E., et al. 2002, ApJ, 573, 7
Fan, X., et al. 2000, AJ, 120, 1167
———. 2001, AJ, 122, 2833
Fardal, M. A., Giroux, M. L., & Shull, J. M. 1998, AJ, 115, 2206
Ferrara, A., Pettini, M., & Shchekinov, Y. 2000, MNRAS, 319, 539
Fields, B. D., Freese, K., & Graff, D. S. 1998, NewA, 3, 347
Giroux, M. L., & Shapiro, P. R. 1996, ApJS, 102, 191
Gnedin, N. Y. 2000, ApJ, 535, 530
Gnedin, N. Y., & Ostriker, J. P. 1997, ApJ, 486, 581
Haiman, Z., Abel, T., & Rees, M. J. 2000, ApJ, 534, 11
Haiman, Z., & Loeb, A. 1997, ApJ, 483, 21
Hernandez, X., & Ferrara, A. 2001, MNRAS, 324, 484
Hu, E. M., Cowie, L. L., McMahon, R. G., Capak, P., Iwamuro, F., Kneib, J.-P., Maihara, T., & Motohara, K. 2002, ApJ, 568, L75
Kriss, G. A., et al. 2001, Science, 293, 1112
Kroupa, P. 2002, Science, 295, 82

Larson, R. B. 1998, MNRAS, 301, 569
Leitherer, C., Ferguson, H. C., Heckman, T. M., & Lowenthal, J. D. 1995, ApJ, 454, L19
Leitherer, C., et al. 1999, ApJS, 123, 3
Madau, P. 1998, in Proc. XVIIIth Moriond Meeting, Dwarf Galaxies and Cosmology, ed. T. X. Thuan, C. Balkowski, V. Cayatte, & J. Trân Thanh Vân (Paris: Editions Frontières), in press (astro-ph/9807200)
Madau, P., Haardt, F., & Rees, M. J. 1999, ApJ, 514, 648
Miralda-Escudé, J. 1998, ApJ, 501, 15
Miralda-Escudé, J., Haehnelt, M., & Rees, M. J. 2000, ApJ, 530, 1
Miralda-Escudé, J., & Ostriker, J. P. 1992, ApJ, 392, 15
Nakamura, F., & Umemura, M. 2002, ApJ, 569, 549
Pryke, C., Halverson, N. W., Leitch, E. M., Kovac, J., Carlstrom, J. E., Holzapfel, W. L., & Dragovan, M. 2002, ApJ, 568, 46
Refregier, A., Rhodes, J., & Groth, E. J. 2002, ApJ, 572, L131
Reiprich, T. H., & Böhringer, H. 2002, ApJ, 567, 716
Ricotti, M., Gnedin, N. Y., & Shull, J. M. 2001, ApJ, 560, 580
———. 2002, ApJ, 575, 49
Schaerer, D. 2002, A&A, 382, 28
Schneider, R., Ferrara, A., Natarajan, P., & Omukai, K. 2002, ApJ, 571, 30
Seljak, U. 2002, MNRAS, submitted (astro-ph/0111362)
Shapiro, P. R., & Giroux, M. L. 1987, ApJ, 321, L107
Shaver, P. A., Hook, I. M., Jackson, C. A., Wall, J. V., & Kellermann, K. I. 1999, in ASP Conf. Ser. 156, Highly Redshifted Radio Lines, ed. C. L. Carilli, S. J. E. Radford, K. M. Menten, & G. I. Langston (San Francisco: ASP), 163

Songaila, A. 2001, ApJ, 561, L153 (erratum 568, L139 [2002])
Spitzer, L. 1978, Physical Processes in the Interstellar Medium (New York: Wiley)
Staggs, S. T., & Church, S. 2001, Report from Snowmass 2001 (astro-ph/0111576)
Steidel, C. C., Pettini, M., & Adelberger, K. L. 2001, ApJ, 546, 665
Tegmark, M., Silk, J., & Blanchard, A. 1994, ApJ, 420, 484
Tegmark, M., Silk, J., Rees, M. J., Blanchard, A., Abel, T., & Palla, F. 1997, ApJ, 474, 1
Tegmark, M., Zaldarriaga, M., & Hamilton, A. J. S. 2001, Phys. Rev. D, 63, 043007
Telfer, R. C., Zheng, W., Kriss, G. A., & Davidsen, A. F. 2002, ApJ, 565, 773
Tumlinson, J., & Shull, J. M. 2000, ApJ, 528, L65
Tumlinson, J., Shull, J. M., & Venkatesan, A. 2003, ApJ, 584, 608 (Paper I)
Valageas, P., & Silk, J. 1999, A&A, 347, 1
Venkatesan, A. 2000, ApJ, 537, 55 (V2000)
———. 2002, ApJ, 572, 15
Venkatesan, A., Giroux, M. L., & Shull, J. M. 2001, ApJ, 563, 1
Wang, X., Tegmark, M., & Zaldarriaga, M. 2002, Phys. Rev. D, 65, 123001
Zhang, P., Pen, U.-L., & Wang, B. 2002, ApJ, 577, 555